Journal of Interdisciplinary Mathematics
ISSN: 0972-0502 (Print), ISSN: 2169-012X (Online)
Vol. 29 (2026), No. 4, pp. 825–840
DOI : 10.47974/JIM-2269

Parameter uniform numerical scheme for singularly perturbed time-fractional delay parabolic reaction-diffusion problems

Feyisa Edosa Merga *
Gemechis File Duressa ‡
Department of Mathematics
Jimma University
Main Campus
Jimma 378
Oromia
Ethiopia

Vishnu Narayan Mishra †
Department of Mathematics
Faculty of Science
Indira Gandhi National Tribal University
Lalpur
Amarkantak 484887
Madhya Pradesh
India

Laxmi Mishra §
Department of Mathematics
National Instutute of Technology
Chaltlang
Aizawl 796012
Mizoram
India

---

* *ORCID-ID:* 0000-0002-8737-8684
‡ *ORCID-ID:* 0000-0003-1889-4690
† *ORCID-ID:* 0000-0002-2159-7710
§ *ORCID-ID:* 0000-0002-2659-7568

---

* *E-mail:* feyisae.2014@gmail.com (Corresponding Author)
‡ *E-mail:* gammeef@gmail.com
† *E-mail:* vishnunarayanmishra@gmail.com
§ *E-mail:* laxmirathour817@gmail.com

Abstract

This work focuses on the numerical solution of a singularly perturbed time-fractional parabolic delay reaction-diffusion problem using a fitted B-spline collocation technique. Applying the Caputo fractional derivative sense, an implicit Euler's technique is used to discretize the time direction. The space direction is handled by a fitted B-spline collocation technique. An established convergence analysis of the method demonstrates that the proposed method attains $O(h^2 + (\Delta t^{2-\alpha}))$ accuracy. The effectiveness of the study is examined through the investigation of two model examples. The results produced by tables and figures show that the scheme is uniformly convergent and possesses two layers near the end of the space domain.

Subject Classification: *26A33, 65M06, 65M12.*

Keywords: *Reaction-diffusion, Time-fractional, Fitted B-spline collocation, Convergence analysis.*

1. Introduction

Differential equations via fractional derivatives, which are an extension of conventional integer-order derivatives, are known as fractional partial differential equations. It offers a great tool for characterizing memory and inherent characteristics of different material and procedures. Scientific and engineering domains, as well as numerous other fields like fluid mechanics, chemistry, viscoelasticity, finance and physics,often utilized fractional partial differential equations [1-5]. For unconventional systems, time-fractional involves unusual diffusion processes that have a temporal component. Subsequently, these kinds of problems are difficult to solve analytically; numerical techniques are employed to approximate the solutions. Fractional differential equations been the subject of numerous computational approaches that have been generated to approximate the solution because of their capacity to simulate complicated processes [6-8].

The mathematical representation of oil reservoir simulations, flow of fluid in porous media, global water production, and several other organic occurrences have been extensively investigated using time-fractional reaction-diffusion equations [9]. Such problems are hard to solve precisely because they are part of an arbitrary order. Therefore, it becomes increasingly crucial to identify reliable and effective numerical strategies for solving such issues numerically. In the papers [10-13], time-fractional reaction-diffusion attempts have been made.

This study focuses on singularly perturbed time-fractional delay parabolic reaction-diffusion problem (SPTFDPRDPs) in the realm $D = D_w \times D_t = (0,1) \times (0,T]$; $\overline{D} = \overline{D}_w \times \overline{D}_t = [0,1] \times [0,T]$; $\Omega = \Omega_L \times \Omega_b \times \Omega_R$ where $\Omega_b = \overline{D}_t \times [-\tau, 0], \Omega_L = \{(0,t): t \in \overline{D}_t\}$ and $\Omega_R = \{(1,t): t \in \overline{D}_t\}$:

$$\left(\frac{\partial^\alpha}{\partial t^\alpha}\kappa - \varepsilon\frac{\partial^2\kappa}{\partial w^2} + b(w)\kappa\right)(w,t) + q(w,t)\kappa(w,t-\tau) = f(w,t);\ (w,t) \in D \quad (1)$$

with initial condition

$$\kappa(w,t) = \varphi_b(w,t), (w,t) \in \Omega_b \quad (2)$$

and the boundary conditions

$$\kappa(0,t) = \varphi_L(t), t \in \Omega_L \text{ and } \kappa(1,t) = \varphi_R(t);\ t \in \Omega_R \tag{3}$$

where $b(w) \geq \vartheta > 0$ is a uninterrupted function, τ is the delay parameter, and $0 < \varepsilon < 1$. The initial boundary value issue yields a distinct result $\kappa(w,t)$ when the functions $b(w), q(w,t), \varphi_b(w,t), \varphi_R(t), \varphi_L(t)$, and $f(w,t))$ fulfill the necessary coherence and regularity conditions. Within the bounds of $w = 0$ and $w = 1$, this remedy displays two boundary layers with thicknesses of $O(\sqrt{\varepsilon})$.

An order of differential equations reduces to $\varepsilon \to 0$ when dealing with parameter dependent delay parabolic reaction-diffusion problems, and the differential equation solution is invariably characterized by an immense gradient [14]. When using conventional traditional computational methods on an even grid, significant oscillation could happen with respect to the behavior of the boundary layer as the perturbation parameter approaches nil over the whole areas of concern. To avoid significant fluctuations, an efficient computational technique with precision apart from the perturbation parameter is going to be utilized. To solve one-dimensional (1D) SPPRDPs with time-lag, a lot of work has been put into developing numerical methods [15-22].

Numerous numerical problems, such as reaction-diffusion problems [24] and unsteady though porous media [23], are addressed by the cubic spline collocation approach. To tackle the initial boundary value issues of the 1D SPTFDPRDPs, the fitted cubic B-spline collocation technique is proposed in this paper.

This research has a particular framework: In Section 2, preliminary data and attributes of continuous solutions are examined. Convergence analysis and numerical formulation are covered Parts three and four as well as parts 5 and 6 offer a summary of the outcomes and computing outcomes, respectively.

2. Preliminaries and Continuous Solution Properties

Definition 1: Let's say that $J \in \mathbb{C}$ and $Re(J) > 0$. The function that represents

$$\Gamma(J) = \int_0^\infty e^{-w} w^{J-1} ds$$

it involves the gamma function.

Definition 2: The expression for a function $\kappa(w,t)$'s Caputo fractional differentiation with regards to t is

$$\frac{\partial^\alpha}{\partial t^\alpha}\kappa(w,t) = \begin{cases} \frac{1}{\Gamma(k-\alpha)} \int_0^t \frac{\partial^k \kappa(w,\zeta)}{\partial \zeta^k} (t-\zeta)^{k-\alpha-1} d\zeta; & \text{if } \alpha \in (k-1,k) \\ \frac{\partial^k \kappa(w,t)}{\partial t^k}; & \text{if } \alpha = k \end{cases}$$

Lemma 1: *Considering that $h \in C^1[0,1]$, let $0 < t_0 < 1$ represent the function's least feasible result. Subsequently,*

$$\partial_c^\alpha h(t_0) \leq \frac{t_0^\alpha}{\Gamma(1-\alpha)}(h(t_0) - h(0)) \leq 0,$$

where, $0 < \alpha < 1$ and ∂_c^α stands for the Caputo fractional derivative.

Proof: The proof is shown on [25]

Lemma 2: *Considering $(w,t) \in C^0(\overline{D})$, suppose $\kappa \in C^2(D) \cap C^0(\overline{D})$. Based on the assumption that $\kappa \geq 0$ on $\partial D = \overline{D} - D$, $\mathcal{L}_\varepsilon \kappa \geq 0$ in D results $\kappa \geq 0$ in $\overline{D}$.*

Proof: Consider a point (ν, ι) that satisfies

$$\chi(\nu,\iota) = \min_{(w,t)\in\overline{D}} \xi(r,t)$$

and $\chi(\nu,\iota) < 0$. Then $\chi(\nu,\iota) \notin \partial D$. Thus,

$$\mathcal{L}_\varepsilon \chi(\nu,\iota) = \chi_{\nu\nu}(\nu,\iota) - b(\nu,\iota)\chi(\nu,\iota) - \frac{\partial^\alpha \chi(\nu,\iota)}{\partial t^\alpha} \leq 0$$

For $\chi_{ww}(\nu,\iota) \geq 0$ and $\frac{\partial^\alpha \chi(\nu,\iota)}{\partial t^\alpha} = 0$, then $\mathcal{L}_\varepsilon \chi(\nu,\iota) \leq 0$, which defies the initial hypothesis. Therefore, $\chi(\nu,\iota) \geq 0 \; \forall (w,t) \in \overline{D}$.

Lemma 3: *(Stability Estimate)*

If $\kappa(w,t)$ is the solution to the continuous issue of Eq.(1), afterwards

$$\|\kappa(w,t)\| \leq \vartheta^{-1}\|L_\varepsilon \kappa\| + \|\kappa\|_\Omega$$

where, $L_\varepsilon \kappa = D_t^\alpha \kappa - \varepsilon u_{ww} + b(w)\kappa(w,t)$.

Proof: State two barrier functions: $\wp^\pm$ referred to as

$$\Psi^\pm(r,t) = \vartheta^{-1}\|L_\varepsilon \kappa\| + \|\kappa\|_\Omega \pm \kappa(w,t), (w,t) \in \overline{D}.$$

At boundaries we have

$$\wp^\pm(0,t) = \vartheta^{-1}\|L_\varepsilon \kappa\| + \|\kappa\|_\Omega \pm \varphi_L \geq \|\kappa\|_\Omega + \pm\varphi_L \geq 0$$

$$\wp^\pm(1,t) = \vartheta^{-1}\|L_\varepsilon \kappa\| + \|\kappa\|_\Omega \pm \varphi_R \geq \|\kappa\|_\Omega + \pm\varphi_R \geq 0$$

and also for $(w,t) \in \Omega_b$, we have

$$\wp^\pm(w,t) = \vartheta^{-1}\|L_\varepsilon \kappa\| + \|\kappa\|_\Omega \pm \varphi_b \geq \|\kappa\|_\Omega + \pm\varphi_b \geq 0$$

Furthermore, $\forall (w,t) \in D$, we have

$$\begin{aligned} L_\varepsilon \wp^\pm(w,t) &= D_t^\alpha \wp^\pm(w,t) - \varepsilon \wp^\pm_{ww}(w,t) + b(w)\wp^\pm(w,t) \\ &= b(w)[\vartheta^{-1}\|L_\varepsilon \kappa\| + \|\kappa\|_\Omega] \pm L_\varepsilon \kappa(w,t) \\ &\geq \|L_\varepsilon \kappa\| + \vartheta\|\kappa\|_\Omega \pm L_\varepsilon \kappa(w,t) \\ &\geq \|L_\varepsilon \kappa\| \pm L_\varepsilon \kappa(w,t) \geq 0. \end{aligned}$$

Lemma 4: *Problem (1) solution and associated derivatives fulfills*

$$\left|\frac{\partial^{l+n}\kappa(w,t)}{\partial w^l \, \partial t^n}\right| \leq C\left[1 + \varepsilon^{\frac{-i}{2}}\left(exp(\tfrac{-w}{\sqrt{\varepsilon}}) + exp(\tfrac{-(1-w)}{\sqrt{\varepsilon}})\right)\right]$$

via $0 \leq l + 2n \leq 4$.

Proof: The proof is on [26]

3. Development of Numerical Schemes

3.1 *Time Discretization*

Eq. (1)'s time derivatives is handles by implicit Euler's technique on domain $D_t^M = \{t_j = j\Delta t; j = 0,1,\ldots,M,\}$ with uniform step size Δt, $t_M = T, \Delta t = \frac{T}{M}$, wherein M remains the quantity of grid points oriented along the time. The formula for the grid $[-\tau, T]$ is $D_t^M = \{t_j = j\Delta t; -m \le j \le M\}$.

Within a Caputo concept, time-fractional derivative is entailed. The resulting quadrature formula can therefore be utilized to Eq.(1) at $t = t_{j+1}$ by applying the implicit Euler technique.

$$\begin{aligned}\partial_t^\alpha K(w, t_{j+1}) &= \frac{1}{\Gamma(1-\alpha)} \int_0^{t_{j+1}} \frac{\partial K(w,v)}{\partial v} (t_{j+1} - v)^{-\alpha} dv \\ &= \frac{1}{\Gamma(1-\alpha)} \sum_{n=0}^{j} \left(\frac{K(w,t_{n+1}) - K(w,t_n)}{\Delta t}\right) \int_{t_n}^{t_{n+1}} (t_{j+1} - v)^{-\alpha} dv + e_{\Delta t}^{j+1} \\ &= \eta \frac{1}{\sum_{n=0}^{j}} \varpi_n \big(K(w, t_{j-n+1}) - K(w, t_{j-n})\big) + e_{\Delta t}^{j+1},\end{aligned}$$

where,

$\eta = \frac{(\Delta t)^{-\alpha}}{\Gamma(1-\alpha)}$, $\varpi_n = ((n+1)^{1-\alpha} - (n)^{1-\alpha})$ and $e_{\Delta t}^{j+1} = \frac{(\Delta t)}{\Gamma(1-\alpha)} \int_{t_n}^{t_{n+1}} (t_{j+1} - v)^{-\alpha} dv$.

Therefore, the Caputo fractional derivative $\partial_t^\alpha \kappa(w, t)$ at the point (w, t_{j+1}) is estimated as

$$\partial_t^\alpha K(w, t_{j+1}) = \eta \left(\big(K(w, t_{j+1}) - K(w, t_j)\big) + \sum_{n=1}^{j} \varpi_n \big(K(w, t_{j-n+1}) - K(w, t_{j-n})\big) \right) \tag{4}$$

We obtain the temporal semi-discrete equation through incorporating Eq. (5) into (1).

$$\begin{aligned}&\eta \left(\frac{K(w,t_{j+1}) - K(w,t_j)}{2^{1-\alpha}} + \sum_{n=1}^{j} \varpi_n \left(K_w^{t_{j-n+1}} - K_w^{t_{j-n}}\right)\right) - \varepsilon K_{ww}^{j+1}(w) + b(w) K^{j+1}(w) \\ &= f^{j+1}(w) - \begin{pmatrix} q(w, t_{j+1}) \varphi_b(w, t_{j+1}); j = 0,1,\ldots,m \\ q(w, t_{j+1}) K(w, t_{j-m+1}); j = m+1,\ldots,M \end{pmatrix}\end{aligned} \tag{5}$$

Aligning Eq. (5) yields

$$(\eta + \mathcal{L}_\varepsilon^{\Delta t}) K^{j+1}(w) = R_i \tag{6}$$

where,

$$(\eta + \mathcal{L}_\varepsilon^{\Delta t}) K^{j+1}(w) = -\varepsilon K_{ww}^{j+1}(w) + (\beta + b(w)) K^{j+1}(w)$$

$$R_i = \begin{cases} \left(\eta K^j + f^{j+1} - q^{j+1} \varphi_b(t_{j+1}) - \eta \sum_{n=1}^{j} \varpi_n (K^{j-n+1} - K^{j-n})\right)(w); j = 0,1,\ldots,m \\ \left(\eta K^j + f^{j+1} - q^{j+1} K^{j-m+1} - \eta \sum_{n=1}^{j} \varpi_n (K^{j-n+1} - K^{j-n})\right)(w); j = m+1,\ldots,M \end{cases}$$

Lemma 5: *The bounded value of an error R in (6) is*

$$\left|e^{j+1}\right| \le C(\Delta t)^{(2-\alpha)}$$

Proof:

$$
\begin{aligned}
e^{j+1} &= \frac{O(\Delta t)}{\Gamma(1-\alpha)} \sum_{n=0}^{j} \int_{t_n}^{t^{n+1}} \left(t_{j+1}-v\right) dv \\
&= \frac{O(\Delta t)}{\Gamma(1-\alpha)} \sum_{n=1}^{j} \left(\frac{(j-n+1)^{1-\alpha}-(j-n)^{1-\alpha}}{1-\alpha}\right) (\Delta t)^{1-\alpha} \\
&= \frac{O((\Delta t)^{2-\alpha})}{\Gamma(2-\alpha)} ((j-n+1)^{1-\alpha}-(j-n)^{1-\alpha}) \\
&= \frac{O((\Delta t)^{2-\alpha})}{\Gamma(2-\alpha)} ((j+1)^{1-\alpha}) \\
&\le C(\Delta t)^{2-\alpha}.
\end{aligned}
$$

Thus,

$$\left|e^{j+1}\right| \le C(\Delta t)^{(2-\alpha)}$$

with C be number that does not depend on ε and Δt.

3.2 Space Discretization

Employing the phase length $h = w_{i+1} - w_i = \frac{1}{N}; i = 0,1,\dots,N-1$, we discretize the spatial derivative by dividing the interval equally in the manner $0 = w_0 < w_1 <\dots< w_N = 1$ as a uniform split of the solution domain $0 \le w \le 1$.

The basis function utilized by the cubic B-spline collocation method $\underline{B_i}(w)$ is outlined as follows:

$$
\underline{B_i}(w) = \frac{1}{h^3}
\begin{cases}
(w-w_{i-2})^3, & w_{i-2} \le w \le w_{i-1}, \\
h^3 + 3h^2(w-w_{i-1}) + 3h(w-w_{i-1})^2 - 3(w-w_{i-1})^3, & w_{i-1} \le w \le w_i, \\
h^3 + 3h^2(w_{i+1}-w) + 3h(w_{i+1}-w)^2 - 3(w_{i+1}-w)^3, & w_i \le w \le w_{i+1}, \\
(w_{i+2}-w)^3, & w_{i+1} \le w \le w_{i+2}, \\
0, & otherwise
\end{cases}
\tag{7}
$$

Table 1 displays $\underline{B_i}(w)$ values as well as the first and second derivatives at the knot points $w_{i-2}, w_{i-1}, w_i, w_{i+1}$, and w_{i+2}.

Table 1

Cubic B-splines coefficients

r	w_{i-2}	w_{i-1}	w_i	w_{i+1}	r_{i+2}
$\underline{B_i}(w)$	0	1	4	1	0
$\underline{B_i'}(w)$	0	$3/h$	0	$-3/h$	0
$\underline{B_i''}(w)$	0	$6/h^2$	$-12/h^2$	$6/h^2$	0

Consider the B-spline interpolating function $\Xi(w)$ for the approximation of $K(w, t_{j+1})$ provided by:

$$\Xi(w) \approx \sum_{i=-1}^{N+1} \gamma_i \underline{B_i}(w) \tag{8}$$

where the unknown parameter γ_i along side the boundary and initial conditions have to be found using the collocation method. ,

Using Eq.(9) and Table 1 an estimate of Ξ_i and associated two initial derivatives are given below:

$$\begin{cases} \Xi_i = \gamma_{i-1} + 4\gamma_i + \gamma_{i+1} \\ \Xi_i' = \frac{3}{h}(\gamma_{i+1} - \gamma_{i-1}) \\ \Xi_i'' = \frac{6}{h^2}(\gamma_{i-1} - 2\gamma_i + \gamma_{i+1}) \end{cases} \tag{9}$$

Thus, by replacing Eq. (7) with Eq. (10), we obtain the following:

$$-\frac{6\varepsilon}{h^2}\left(\gamma_{i-1}^{j+1} - 2\gamma_i^{j+1} + \gamma_{i+1}^{j+1}\right) + (\eta + b_i)\left(\gamma_{i-1}^{j+1} + 4\gamma_i^{j+1} + \gamma_{i+1}^{j+1}\right) = \bar{R}_i \tag{10}$$

In order to regulate the impact of a singular perturbation parameter regarding to the behavior of solution, we add an artificial viscosity $\sigma(w_i, \varepsilon)$ to equation (11). As a result we get:

$$\left(-\frac{6\sigma_i}{h^2} + \eta + b_i\right)\gamma_{i-1}^{i+1} + \left(\frac{12\sigma_i}{h^2} + 4\eta + 4b_i\right)\gamma_i^{j+1} + \left(-\frac{6\sigma_i}{h^2} + \eta + b_i\right)\gamma_{i+1}^{j+1} = \bar{R}_i. \tag{11}$$

The determination of an artificial viscosity σ_i is necessary to guarantee which Eq. (12)'s outcome matches evenly toward the exact outcomes of Eq. (1).

Eq.(12) is therefore a systems of linear equations of order $(N + 3) \times (N + 3)$, expressed as a three term recurrence relation of the following form:

$$E_i\gamma_{i-1}^{j+1} + F_i\gamma_i^{j+1} + G_i\gamma_{i+1}^{j+1} = H_i;\ i = 0,1,\ldots,N \tag{12}$$

where;

$$E_i = G_i = -6\sigma_i + (\eta + b_i)h^2$$
$$F_i = 12\sigma_i + 4(\eta + b_i)h^2$$
$$H_i = h^2\bar{R}_i$$

and

$$\sigma_i = \frac{h^2 b_i}{6}\left(\frac{1+2cosh^2(\rho_i h)}{2sinh^2\rho_i h}\right);\ \rho_i = \sqrt{\frac{b_i}{\varepsilon}}$$

for $|\sigma_i - \varepsilon| \le Ch^2$ with C is independent of ε and h [21, 27].

By applying the boundary conditions (3) to Eq.(10), we may reduce the order of systems of linear equations, yielding

$$\begin{aligned} \gamma_{-1} &= \varphi(t_{j+1}) - 4\gamma_0 - \gamma_1 \\ \gamma_{N+1} &= \phi(t_{j+1}) - \gamma_{N-1} - 4\gamma_N \end{aligned} \tag{13}$$

Eq.(14) is now incorporated into Eq.(13) to produce $(N + 1) \times (N + 1)$ systems of linear equation:

$$\begin{aligned}&(F_0-4E_0)\gamma_0^{j+1}+(G_0-E_0)\gamma_1^{j+1}=H_0-E_N\varphi(t_{j+1})\\&E_i\gamma_{i-1}^{j+1}+F_i\gamma_i^{j+1}+G_i\gamma_{i+1}^{j+1}=H_i;\quad i=,1,\ldots,N-1\\&(E_N-G_N)\gamma_{N-1}^{j+1}+(F_N-4G_N)\gamma_N^{j+1}=H_N-G_N\phi(t_{j+1}).\end{aligned}\tag{14}$$

Convergence analysis

Lemma 6: *The cubic B-spline collocation* $\{\underline{B}_{-1}(w),\underline{B}_0(w),\ldots,\underline{B}_N(w),\underline{B}_{N+1}(w)\}$*, as given in (8) fulfills the inequality*

$$\sum_{i=-1}^{N+1}\left|\underline{B}_i(w)\right|\le 10;\ w\in[0,1]\tag{15}$$

Proof: Triangular inequality gives rise to

$$\left|\sum_{i=-1}^{N+1}\underline{B}_i(w)\right|\le\sum_{i=-1}^{N+1}\left|\underline{B}_i(w)\right|$$

At just three nodal points does the cubic B-spline $\underline{B}_i(w)$ exhibit non-zero values.

At any node r_i, we have

$$\sum_{i=-1}^{N+1}\left|\underline{B}_i(w)\right|=\left|\underline{B}_{i-1}(w)\right|+\left|\underline{B}_i(w)\right|+\left|\underline{B}_{i+1}(w)\right|=1+4+1=6<10$$

For $r\in[w_{i-1},w_i]$

$$\sum_{i=-1}^{N+1}\left|\underline{B}_i(w_i)\right|\le 4 \text{ and } \sum_{i=-1}^{N+1}\left|\underline{B}_{i-1}(w_{i-1})\right|\le 4$$

and similarly for $w\in[w_{i-1},w_i]$

$$\sum_{i=-1}^{N+1}\left|\underline{B}_{i+1}(w_i)\right|\le 1 \text{ and } \sum_{i=-1}^{N+1}\left|\underline{B}_{i-2}(w_{i-1})\right|\le 1$$

Therefore, for any point $r\in[w_{i-1},w_i]$, we obtain

$$\sum_{i=-1}^{N+1}\left|\underline{B}_i(w)\right|=\left|\underline{B}_{i-2}(w)\right|+\left|\underline{B}_{i-1}(w)\right|+\left|\underline{B}_i(w)\right|+\left|\underline{B}_{i+1}(w)\right|\le 10.$$

Lemma 7: *Given the boundary value concerning in (7), let* $\Xi(w)$ *denote the collocation estimate of the solution* $\bar{\kappa}(w)$ *at the* $(j+1)$*-th time step. For* $R\in C^2[0,1]$*, consequently the* ε*-uniform error approximation could be obtained as*

$$\|\bar{\kappa}(w_i)-\Xi(w_i)\|_\infty\le C(h^2)\tag{16}$$

for h *to be small enough and* C *to be positive.*

Proof: For the boundary value issue (7), let $\bar{\Xi}(w)$ be a unique spline that interpolate $\bar{\kappa}(w)$ at the $(j+1)^{th}$ time level, which is provided via

$$\bar{\Xi}(w)\approx\sum_{i=-1}^{N+1}\bar{\gamma}_i\underline{B}_i(w)\tag{17}$$

If $b(w),R_i\in C^2[0,1]$, then $\bar{\kappa}(w)\in C^4[0,1],\forall j;0\le j\le M$ and hence from error bound estimate [28] we get

$$\|D^n(\bar{\kappa}(w)-\bar{\Xi}(w))\|_\infty\le\varsigma_n\left\|\frac{d^4\bar{\kappa}(w)}{dw^4}\right\|_\infty h^{4-k};\ k=0,1,2,\tag{18}$$

and ς_k is constant independent of term h and N.

Using triangular inequality we have

$$\|\bar{\kappa}(w_i)-\Xi(w_i)\|_\infty\le\|\bar{\kappa}(w_i)-\bar{\Xi}(w_i)\|_\infty+\|\bar{\Xi}(w_i-\Xi(w_i)\|_\infty.\tag{19}$$

Let $\left(\eta+\mathcal{L}_{\varepsilon}^{\Delta t,h}\right)\Xi(w_i)=\left(\eta+\mathcal{L}_{\varepsilon}^{\Delta t,h}\right)\bar{\kappa}(w_i)=H_i$, assume also $\left(\eta+\mathcal{L}_{\varepsilon}^{\Delta t,h}\right)$ $\bar{\Xi}(w_i)=\bar{H}_i$ that fulfills the boundary requirements $\bar{\Xi}(w_0)=\varphi(t_{j+1})$ and $\bar{\Xi}(w_N)=\phi(t_{j+1})$. Then,

$$\begin{aligned}&\left|\left(\eta+\mathcal{L}_{\varepsilon}^{\Delta t,h}\right)\bar{\kappa}(w_i)-\left(\eta+\mathcal{L}_{\varepsilon}^{\Delta t,h}\right)\bar{\Xi}(w_i)\right|=\left|\left(\eta+\mathcal{L}_{\varepsilon}^{\Delta t,h}\right)\Xi(w_i)-\left(\eta+\mathcal{L}_{\varepsilon}^{\Delta t,h}\right)\bar{\Xi}(w_i)\right|\\&=\left|-\varepsilon\frac{d^2\bar{\kappa}(w_i)}{dw^2}-\left(-\sigma_i\frac{d^2\bar{\Xi}(w_i)}{dw^2}\right)+b(w_i)(\bar{\kappa}(w_i)-\bar{\Xi}(w_i))\right|\\&\leq|\sigma_i-\varepsilon|\varsigma_2\left\|\frac{d^2u\bar{\kappa}(w_i)}{dw^2}\right\|_\infty+|\varepsilon|\varsigma_2\left\|\frac{d^2\bar{\kappa}(w_i)}{dw^2}\right\|_\infty+\\&\quad\varsigma_0\|b(w_i)\|_\infty\|\bar{\kappa}(w_i)\|_\infty.\end{aligned}\tag{20}$$

We now have $|\sigma_i-\varepsilon|\leq Ch^2$ from the bound of artificial viscosity. Putting this and Lemma 4 into Eq.(21) allows as to obtain

$$\max_{w\in D}\left|\left(\eta+\mathcal{L}_{\varepsilon}^{\Delta t,h}\right)\bar{\kappa}(w_i)-\left(\eta+\mathcal{L}_{\varepsilon}^{\Delta t,h}\right)\bar{\Xi}(w_i)\right|\leq\varsigma h^2,\tag{21}$$

where $\varsigma=\varepsilon\varsigma_2+(C\varsigma_2+\varsigma_0\|b(w_i)\|_\infty)h^2$.

By combining the unique interpolate approximation (18) and recurrence relation (13) the i-th coordinate of $\left|\left(\eta+\mathcal{L}_{\varepsilon}^{\Delta t,h}\right)(\bar{\kappa}(w_i)-\bar{\Xi}(w_i))\right|$ yields

$$36\sigma_0\mu_0=Y_0\tag{22}$$

$$\begin{aligned}&(-6\sigma_i+h^2(\eta+b_i^{j+1}))\mu_{i-1}+(12\sigma_i+4h^2(\eta+b_i))\mu_i+\\&\qquad(-6\sigma_i+h^2(\eta+b_i))\mu_{i+1}=Y_i,i=1,2,\dots,N-1\end{aligned}\tag{23}$$

$$36\sigma_N\mu_N=Y_N\tag{24}$$

where; $\mu_i=\gamma_i-\bar{\gamma}_i; i=-1,0,\dots,N+1$ and $Y_i=H_i-\bar{H}_i; i=0,1,\dots,N$.

Then, inequality (24) results the following

$$|Y_i|\leq h^2|H_i-\bar{H}_i|\leq\varsigma h^4\tag{25}$$

Inequality (24) written as

$$(12\sigma_i+4h^2(\eta+b_i^{j+1}))\mu_i=Y_i-(-6\sigma_i+h^2(\eta+b_i))(\mu_{i-1}+\mu_{i+1}).\tag{26}$$

Let us define

$$Y=\max_{1\leq x\leq N-1}Y_i,\quad \mu=\max_{1\leq x\leq N-1}\mu_i$$

and using the constraint $0<\vartheta\leq b_i$ in Eq.(27) calculating the magnitude and the inequality $|\sigma_i|\leq\varepsilon+Ch^2$ after which we obtain

$$\begin{aligned}(12\varepsilon+(4(\eta+\vartheta)+12C)h^2)\mu&=Y+2\mu(6\varepsilon-(\eta+\vartheta-6C)h^2)\\&\leq Y+2\mu(6\varepsilon+(\eta+\vartheta+6C)h^2).\end{aligned}$$

By simplifying this, we can get

$$2\mu(\eta+\vartheta)h^2\leq Y\leq\varsigma h^4$$

which gives

$$\mu\leq\frac{\varsigma h^2}{(\eta+\vartheta)}.$$

With the same instances

$$\mu_0\leq\frac{\varsigma h^2}{36C},\mu_N\leq\frac{\varsigma h^2}{36C}.$$

Once more, μ_{-1} and μ_{N+1} values are determined using the boundary condition (14) that we possess

$$\mu_{-1} \leq \varsigma h^2 \left(\frac{1}{9C} + \frac{1}{C(\eta+\vartheta)}\right), \mu_{N+1} \leq \varsigma h^2 \left(\frac{1}{9C} + \frac{1}{C(\eta+\vartheta)}\right).$$

Accordingly, using the values of $\varsigma = \varepsilon\varsigma_2 + \left(C\varsigma_2 + \varsigma_0\left\|b(w_i, t_{j+1})\right\|_{\infty}\right)h^2$, there exists a number ρ , that doesn't depend on h or ε such that

$$\mu = \max_{-1\leq w\leq N+1}\{\mu_i\} \leq \rho h^2. \tag{27}$$

Lemma 6 and inequality (28) give us

$$\Xi(w_i) - \bar{\Xi}(w_i) = \sum_{i=-1}^{N+1} (\gamma_i - \bar{\gamma}_i)\underline{B_i}(w)$$

$$\|\Xi(w_i) - \bar{\Xi}(w_i)\|_{\infty} \leq 10\rho h^2. \tag{28}$$

As a result, considering the triangular inequality, we arrive at

$$\|\bar{\kappa}(w_i) - \Xi(w_i)\|_{\infty} \leq Ch^2$$

where, $C = 10\rho + \varsigma_0 h^2$.

Theorem 8: *Assuming that equation (1) has a solution of $\kappa(w,t)$, the discretized equation as a whole has a solution of $\kappa(w_i, t_{j+1})$. The ε −uniform bound given in Lemma 5 and 7 is valid*

$$\max_{0\leq i,j\leq N,M-1}\left|\kappa(w_i, t_{j+1}) - \Xi(w_i)\right| \leq C(h^2 + (\Delta t)^{2-\alpha}) \tag{29}$$

here C represents a number that is not affected by ε, h and (Δt).

Proof: Triangle inequality is employed in the demonstration.

5. Numerical Results

Due the following numerical examples has lack of analytical solutions, we implemented the double mesh principles to enhance the accuracy. Point-wise maximum absolute error $E_{N,M}$ and numerical solution $(N.S)$ of the numerical examples are displayed in tables and figures, respectively.

Example 1:

$$\frac{\partial^\alpha \kappa(w,t)}{\partial t^\alpha} - \varepsilon\frac{\partial^2 \kappa(w,t)}{\partial w^2} + (1.1 + w^2)\kappa(w,t) + \kappa(w, t-\tau) = t^3$$

with regard to the constraints

$$\kappa(w,0) = 0, (w,t) \in [0,1] \times [-1,0]$$

and

$$\kappa(0,t) = 0 = u(1,t) = 0;\ t \in [0,2]$$

Example 2:

$$\frac{\partial^\alpha \kappa(w,t)}{\partial t^\alpha} - \varepsilon\frac{\partial^2 \kappa(w,t)}{\partial w^2} + \frac{(1+w)^2}{2}\kappa(w,t) + \kappa(w, t-\tau) = t^3$$

with regard to the constraints

$$\kappa(w,0) = 0, (w,t) \in [0,1] \times [-1,0]$$

and

$$\kappa(0,t) = 0 = \kappa(1,t) = 0;\ t \in [0,2]$$

Table 2

$E_{N,M}$ **for various values of** α **and certain** $\varepsilon = 10^{-10}$ **of Ex:1**

α	N=32, M=4	N=64, M=8	N=128, M=16	N=256, M=32
0.25	8.3706e-03	1.8584e-03	1.6576e-03	2.3660e-03
0.50	2.4337e-02	7.6181e-03	2.7567e-03	2.5023e-03
0.75	4.5923e-02	1.9759e-02	7.7090e-03	3.2068e-03
0.90	6.0623e-02	2.9544e-02	1.3620e-02	6.0854e-03

Table 3

$E_{N,M}$ **of Ex:1 for** $\alpha = 0.8$

ε	N=32, M=4	N=64, M=8	N=128, M=16	N=256, M=32
10^{0}	7.2980e-03	3.3896e-03	1.3837e-03	5.9253e-04
10^{-2}	8.1229e-03	3.5708e-03	1.4262e-03	6.0286e-04
10^{-4}	7.9054e-02	2.1391e-02	5.6838e-03	1.6416e-03
10^{-8}	5.0700e-02	2.2861e-02	9.4473e-03	3.9001e-03
10^{-10}	5.0700e-02	2.2861e-02	9.4473e-03	3.9008e-03
10^{-12}	5.0700e-02	2.2861e-02	9.4473e-03	3.9008e-03
10^{-14}	5.0700e-02	2.2861e-02	9.4473e-03	3.9008e-03
10^{-16}	5.0700e-02	2.2861e-02	9.4473e-03	3.9008e-03
$E^{N,M}$	5.0700e-02	2.2861e-02	9.4473e-03	3.9008e-03
$r^{N,M}$	1.1491	1.2749	1.2761	

Table 4

$E_{N,M}$ **for various values of** α **and certain** $\varepsilon = 10^{-10}$ **of Ex:2**

α	N=32, M=4	N=64, M=8	N=128, M=16	N=256, M=32
0.25	1.5231e-02	3.4973e-03	2.9007e-03	4.1405e-03
0.50	4.1145e-02	1.3296e-03	4.7024e-03	3.9683e-03
0.75	7.2576e-02	3.0790e-02	1.2015e-02	4.9228e-03
0.90	9.2936e-02	4.3367e-02	1.9582e-02	8.6701e-03

Table 5

$E_{N,M}$ **of Ex:2 for** $\alpha = 0.8$

ε	N=32, M=4	N=64, M=8	N=128, M=16	N=256, M=32
10^{0}	4.9265e-03	2.2812e-03	9.2841e-04	4.0034e-04
10^{-2}	5.6293e-03	2.4400e-03	9.6596e-04	4.0955e-04
10^{-4}	7.6395e-02	1.8703e-02	4.7957e-03	1.3424e-03
10^{-8}	7.9238e-02	3.4880e-02	1.4321e-02	2.4778e-03
10^{-10}	7.9238e-02	3.4880e-02	1.4327e-02	5.8704e-03
10^{-12}	7.9238e-02	3.4880e-02	1.4327e-02	5.8704e-03
10^{-14}	7.9238e-02	3.4880e-02	1.4327e-02	5.8704e-03
10^{-16}	7.9238e-02	3.4880e-02	1.4327e-02	5.8704e-03
$E^{N,M}$	7.9238e-02	3.4880e-02	1.4327e-02	5.8704e-03
$r^{N,M}$	1.1838	1.2837	1.2872	

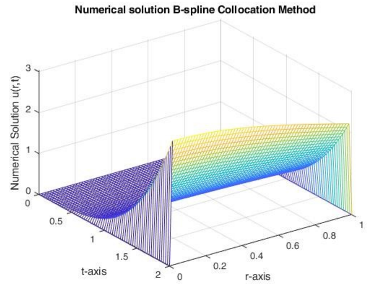

Figure 1
$(N.S)$ of Ex:1 for $N = M = 64$ and $\varepsilon = 10^{-10}$

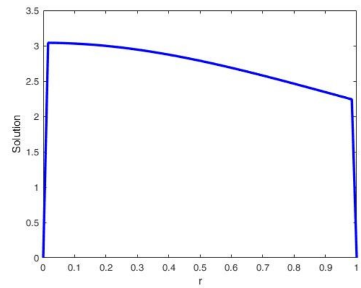

Figure 2
Formation of the boundary layer of Ex:1

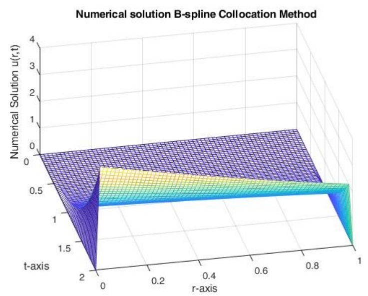

Figure 3
$(N.S)$ of Ex:2 for $N = M = 64$ and $\varepsilon = 10^{-10}$

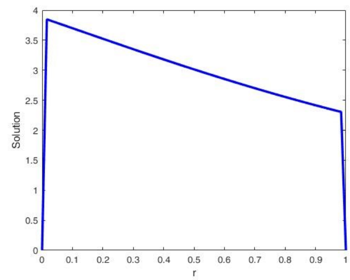

Figure 4
Formation of the boundary layer of Ex:2

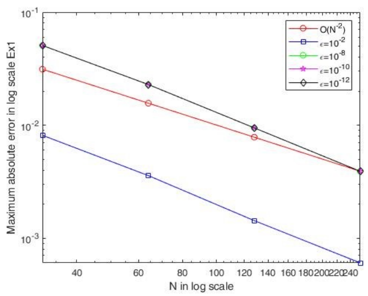

Figure 5
log?log structure for Ex:1

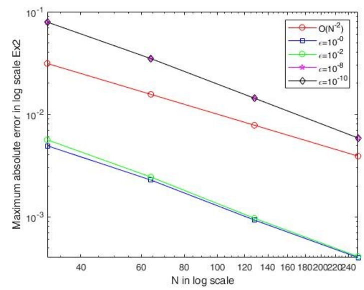

Figure 6
log?log structure for Ex:2

A fitted cubic B-spline collocation approach is engaged for problems 1 and 2 for verifying the assumptions made in theory. For various values of α and fixed

ε, the maximum absolute errors can be found in Tables 2 and 4. Maximum absolute error decreases as well as α does, as can be seen in the tables, revealing that the fractional order model more accurately captured actual life issues compared to the representation of integer order. Tables 3 and 5 illustrate the test examples point-wise maximum absolute errors. The tables demonstrate that the results of the numerical examples converge uniformly as the quantity of mesh measurements rises and the perturbation parameter nears zero. Figures 1 and 3 depict the scheme of physical behavior and provide a numerical illustration with a twin layer at the end of the space domain. A parabolic boundary layer can potentially be visible at $w = 0$ and $w = 1$ in figures 2 and 4, which exhibit the boundary layer behavior. Furthermore, the log-log level of the highest absolute error is depicted in figures 5 and 6. It indicated the maximum absolute error falls monotonically as the number of grid points grows and $\varepsilon \to 0$, confirming a consensus with theoretical results.

6. Conclusions

In this study, the 1D SPTFDPRDPs are investigated and treated by implicit Euler's technique on top of Caputo sense in the time domain. The space domain is discretized by the fitted B-spline collocation method. Following an extensive convergence analysis, it was shown that the suggested numerical method attains an order of accuracy of $O(h^2 + (\Delta t)^{2-\alpha})$. The numerical findings are further supported by numerical examples, demonstrating a good agreement between the anticipated results and numerical outcomes. These examples demonstrate that the suggested approach accurately depicts the characteristics of the solution, regardless of the presence of the boundary layers at $w = 0$ and $w = 1$.

Conflict Interest and Financial Disclose

The author reveal there is no conflict of interests and no funding is provided for this work.

References

[1] R. L. Bagley and P. J. Torvik, "A theoretical basis for the application of fractional calculus to viscoelasticity," *Journal of Rheology*, vol. 7, no. 3, pp. 201–210 (1983).

[2] D. A. Benson, S. W. Wheatcraft, and M. M. Meerschaert, "Application of a fractional advection-dispersion equation," *Water Resources Research*, vol. 36, no. 6, pp. 1403–1412 (2000).

[3] R. Choudhary, S. Singh, and D. Kumar, "A second-order numerical scheme for the time-fractional partial differential equations with a time delay," *Computational and Applied Mathematics*, vol. 41, no. 3, Art. no. 114 (2022).

[4] A. D. Fitt, A. R. H. Goodwin, K. A. Ronaldson, and W. A. Wakeham, "A fractional differential equation for a MEMS viscometer used in the oil industry," *Journal of Computational and Applied Mathematics,* vol. 229, no. 2, pp. 373–381 (2009).

[5] M. Oeser and S. Freitag, "Modeling of materials with fading memory using neural networks," *International Journal for Numerical Methods in Engineering*, vol. 78, no. 7, pp. 843–862 (2009).

[6] A. A. Kilbas, H. M. Srivastava, and J. J. Trujillo, *Theory and Applications of Fractional Differential Equations*. Amsterdam, The Netherlands: Elsevier, vol. 204 (2006).

[7] C. Jadhav, T. Dale, and S. Dhondge, "A review on applications of fractional differential equations in engineering domain," *Materials Science and Engineering: Advances*, vol. 71, no. 4, pp. 7147–7166 (2022).

[8] W. T. Aniley and G. F. Duressa, "Nonstandard finite difference method for time-fractional singularly perturbed convection–diffusion problems with a delay in time," *Results in Applied Mathematics*, vol. 21, Art. no. 100432 (2024).

[9] P. Pandey, S. Kumar, J. F. Gómez-Aguilar, and D. Baleanu, "An efficient technique for solving the space–time fractional reaction–diffusion equation in porous media," *Chinese Journal of Physics*, vol. 68, pp. 483–492 (2020).

[10] V. Chuk, B. Datsko, and V. Meleshko, "Mathematical modeling of time-fractional reaction–diffusion systems," *Journal of Computational and Applied Mathematics*, vol. 220, no. 1–2, pp. 215–225 (2008).

[11] J. Zhang and X. Yang, "A class of efficient difference method for time-fractional reaction–diffusion equation," *Computational and Applied Mathematics,* vol. 37, no. 4, pp. 4376–4396 (2018).

[12] K. Van Bockstal, M. A. Zaky, and A. S. Hendy, "On the existence and uniqueness of solutions to a nonlinear variable-order time-fractional reaction–diffusion equation with delay," *Communications in Nonlinear Science and Numerical Simulation*, vol. 115, Art. no. 106755 (2022).

[13] T. Hamadneh, Z. Chebana, I. Abu Falahah, Y. A. Al-Khassawneh, A. Al-Husban, T. E. Oussaeif, and A. Abbes, "On finite-time blow-up problem for nonlinear fractional reaction–diffusion equation: Analytical results and numerical simulations," *Fractal and Fractional*, vol. 7, no. 8, Art. no. 589 (2023).

[14] J. J. Miller, E. O'Riordan, and G. I. Shishkin, Fitted Numerical Methods for Singular Perturbation Problems: Error Estimates in the Maximum

Norm for Linear Problems in One and Two Dimensions. Singapore: World Scientific (1996).

[15] A. R. Ansari, S. A. Bakr, and G. I. Shishkin, "A parameter-robust finite difference method for singularly perturbed delay parabolic partial differential equations," *Journal of Computational and Applied Mathematics*, vol. 205, no. 1, pp. 552–566 (2007).

[16] R. N. Rao and P. P. Chakravarthy, "A fitted Numerov method for singularly perturbed parabolic partial differential equation with a small negative shift arising in control theory," *Numerical Mathematics: Theory, Methods and Applications*, vol. 7, no. 1, pp. 23–40 (2014).

[17] F. W. Gelu and G. F. Duressa, "A uniformly convergent collocation method for singularly perturbed delay parabolic reaction–diffusion problem," *Abstract and Applied Analysis*, vol. 2021, pp. 1–11 (2021).

[18] E. A. Megiso, M. M. Woldaregay, and T. G. Dinka, "Fitted tension spline method for singularly perturbed time-delay reaction–diffusion problems," *Mathematical Problems in Engineering*, vol. 2022, Art. ID (2022).

[19] A. A. Tiruneh, G. A. Derese, and D. M. Tefera, "A nonstandard fitted operator method for singularly perturbed parabolic reaction–diffusion problems with a large time delay," *International Journal of Mathematics and Mathematical Sciences*, vol. 2022, pp. 1–11 (2022).

[20] K. Khari and V. Kumar, "Finite element analysis of the singularly perturbed parabolic reaction–diffusion problems with retarded argument," *Numerical Methods for Partial Differential Equations*, vol. 38, no. 4, pp. 997–1014 (2022).

[21] N. T. Negero, "A robust fitted numerical scheme for singularly perturbed parabolic reaction–diffusion problems with a general time delay," *Results in Physics*, vol. 51, Art. no. 106724 (2023).

[22] J. Howlader, P. Mishra, and K. K. Sharma, "An orthogonal spline collocation method for singularly perturbed parabolic reaction–diffusion problems with time delay," *Journal of Applied Mathematics and Computing*, vol. 70, no. 2, pp. 1069–1101 (2024).

[23] P. Shah, P. Tandel, and J. Prajapati, "A study on unsteady flow through porous media: A cubic spline collocation approach," *Journal of Interdisciplinary Mathematics*, vol. 24, no. 5, pp. 1375–1386 (2021).

[24] S. Natesan and B. S. Deb, "A robust computational method for singularly perturbed coupled system of reaction–diffusion boundary-value problems," *Applied Mathematics and Computation*, vol. 188, no. 1, pp. 353–364 (2007).

[25] W. T. Aniley and G. F. Duressa, "Uniformly convergent numerical method for time-fractional convection–diffusion equation with variable coefficients," *Partial Differential Equations and Applications in Mathematics*, vol. 8, Art. no. 100592 (2023).

[26] E. B. Bashier and K. C. Patidar, "A novel fitted operator finite difference method for a singularly perturbed delay parabolic partial differential equation," *Applied Mathematics and Computation*, vol. 217, no. 9, pp. 4728–4739 (2011).

[27] M. K. Kadalbajoo and P. Arora, "B-spline collocation method for a singularly perturbed reaction–diffusion problem using artificial viscosity," *Journal of Applied Mathematics and Computing*, vol. 6, no. 1, pp. 23–41 (2009).

[28] C. A. Hall, "On error bounds for spline interpolation," *Journal of Approximation Theory*, vol. 1, no. 2, pp. 209–218 (1968).

Received November, 2024